ICA 2022
24th INTERNATIONAL CONGRESS ON ACOUSTICS
October 24(Mon) - 28(Fri), 2022 Gyeongju, Korea

PROCEEDINGS of the
24th International Congress on Acoustics

October 24 to 28, 2022 in Gyeongju, Korea

ABS-0785

System for portable audio-based EEG feature extraction and adaptive playback

Wannes VAN RANSBEECK[(1)], Arthur VAN DEN BROUCKE[(2)], Sarah VERHULST[(3)]

[(1)]Hearing Technology Lab @ WAVES Ghent University, Belgium, wannes.vanransbeeck@ugent.be

[(2)]Hearing Technology Lab @ WAVES Ghent University, Belgium, arthur.vandenbroucke@ugent.be

[(3)]Hearing Technology Lab @ WAVES Ghent University, Belgium, sarah.verhulst@ugent.be

ABSTRACT

The interactions between humans and music are often studied through an impulse-response paradigm where the human response is considered purely a reaction to the present signal, hence neglecting more subtle relations and underlying patterns. In this paper a portable biomonitoring and music playback system will be presented, studying the correlation between humans and music, with a more in-depth focus on analysing and characterising this interaction based on embodiment and bio-feedback. A Raspberry Pi environment is extended with an 8 channel 16kHz ADS-chip, capable of mobile high sample rate capture of EEG data from cEEGrid-electrodes, which holds future extension possibilities to heart rate, saturation and movement. Furthermore, a high amplification is present to allow subcortical signal capture along with adaptive music playback to alter and monitor playback synchronised with data capture. This permits on-board analysis of the music interaction and response-based playback adaptation. The system provides EEG data capture with a 3400Hz 3dB-bandwidth and RMS input-referred noise of 0.503μV. A comparison was made with state-of-the-art cortical capturing devices through an ABR measurement with stationary Biosemi EEG equipment. Additionally, an overview will be presented of the aimed interaction and performance with regard to synchronisation of audio and EEG measurements and their analysis.

Keywords: Bio-feedback, interaction, EEG

1 INTRODUCTION

Stemming from the shown positive sociological, medical and health oriented influence of sound and music on a human being (1, 2, 3, 4), there currently is an omnipresent interest in the characterisation of these interactions (5, 6, 7, 8). For example, their influence has been found to be beneficial for both rehabilitation in general (26) as specifically in treatment of the Parkinson's disease (27, 28), mental diseases (autism spectrum disorder) (29, 30) as well as general well-being (31). Said interactions are evaluated during presentation through bio-markers (EEG, heart rate, saturation, movement and etc.) which then provide a more in-depth view of how the sound is perceived and is responded to (9, 10, 11). However, the response is often considered a pure stimulus response, i.e. a pure one way result of the input. Neglecting then any interaction or more intricate relations which may be present in human-machine or human-human music interactions, as have been reported by mathematician, philosophers, musicologist and other scientists (12, 13, 14). Additionally, motivation in test subjects may be limited due to the lack of interaction potential.

In line with the above reasoning a more human-like **adaptive music playback system**, based on bio-markers, is hence preferred. Although the idea of altering playback based on human response in general is not innovating, as multiple implementations have been made based on brain potentials, heart rate and others (32, 33, 34, 35), their implementations do often not consider the resulting interaction which is realised between both listener and sound or do this to a limited extend. It should however be stated that work by *Dasenbrock et al.* (38) provides a similar feedback aimed implementation as the presented work. However, here a more standalone

system is aimed for playback and capture, suited as well for sub-cortical EEG capture, for example the Auditory Brainstem Response (**ABR**). The latter presenting higher demands on playback together with a more clear emphasis on interaction.

In this paper a proof of concept system (**POC**) is presented, which is aimed at overcoming these limitations by offering a portable and light-weight system for in-depth **real-time analysis** of the interaction as it manifests itself between bio-markers (internally recorded EEG or acquired through I2C or SPI communication) and sound. The analysis here will be based on **spectral** and **temporal** properties of both. The system is furthermore capable of adapting the music playback based on mentioned analysis, thus creating an adaptive loop. In turn, a more human-like interaction between man and machine will be aimed for, better suited for human-like music responses and realising an adaptive engaging environment which can be evaluated in real time.

2 SYSTEM DESIGN

2.1 Hardware layout

The system layout is presented below in Figure 1 and consists of two main components 1) An EEG capture module containing a preamplifier, low pass filters, an ADC and optional capabilities of microphone integration and 2) A central computing Raspberry Pi 3b+ module, for processing, external device communication over I2C and SPI, storage and an audio playback module.

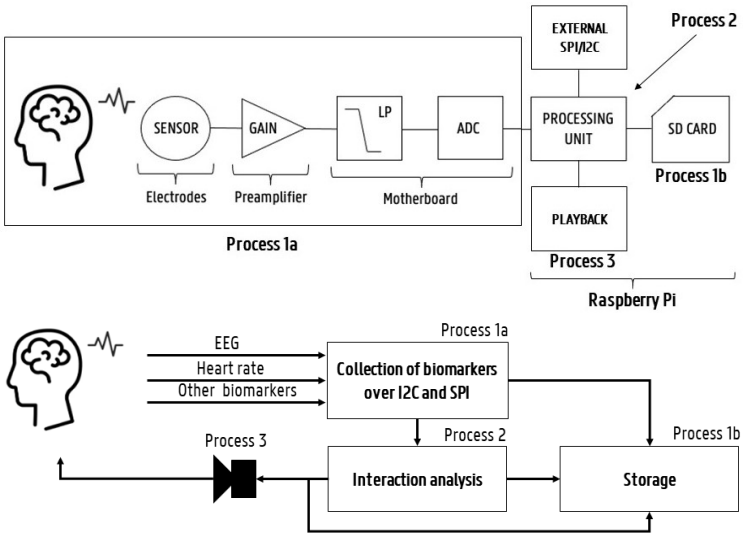

Figure 1. Overview of hardware layout (upper) and data flows (lower) inside the proof of concept system, based on illustrations provided by and used with permission of *Van Den Broucke* (15). *Process 1a)* capture of biomarkers, *Process 1b)* storage of biomarkers, *Process 2)* interaction analysis, *Process 3)* adaptive playback.

2.1.1 EEG capture

The EEG capture and its subcomponents (*Process 1a, Process 1b*), providing signal processing and storage, are shortly discussed below. Additional documentation and evaluation of the EEG capture can be found in (15).

The auditory evoked potentials (EEG) are recorded by cEEGrid electrodes consisting of 8 electrodes placed around the ear, developed by the group of Bleichner and Debener (17, 18). Which, due to their shape and placement, are dedicated to hearing diagnostics and in particular the evaluation of them through the capturing of Envelope Following Response (**EFR**) and ABR signals. Second, the captured activity is amplified through low-noise (7nV/Hz, 3400Hz 3dB bandwidth) preamlifiers with a gain factor of 100, which ensures being capable of capturing subcortical EEG data. The preamplifiers furthermore possess a common mode rejection ratio (CMRR) of -110dB and an offset voltage of 0.5μV and were equipped with a driven-right leg feedback loop to ensure a

proper range for the preamplifiers. Third, the amplified signals are passed onto the motherboard through a low-pass anti-aliasing filter before being processed by a 16kHz analog-to-digital 24bit ADS1299 chip designed for medical instrumentation studies. This also includes portable EEG measurements due to its low cost and power usage (15). An external trigger input can also be provided to the ADS-chip to allow full ABR measurements on the system. A 7.4V, 6000mAh lithium battery was furthermore connected to the motherboard serving as the main power supply during operation for both the motherboard and processing unit.

An overview of the specification of the EEG-system may be found below in Table 1 taken from the in-depth performance analysis and discussion in *Van Den Broucke* (15). It should however be stated that the main processing in the latter paper for EEG-measurement is evaluated and controlled through an ESP32-WROOM-32 (19) chip from the Espressif Company. Alternatively, communication and storage will here be handled through a Raspberry Pi. Nevertheless, this should not influence the actual functioning of the EEG capture.

Table 1. Specification of EEG-system as taken from *Van Den Broucke* (15)

Specification	**System performance**
Maximum sample rate	16000Hz
Sample rate accuracy	< 200ps
Sampling skew	25ps
Bandwidth (-3dB)	3400Hz
Total input ref. noise	0.5μVrms
Harmonic distortion	< 0.001%
Resolution	24bit
CMRR(at 50Hz)	> 110dB

2.2 General interaction system and human

The main processing unit consists of a Raspberry Pi 3B+ from Raspberry Pi (21) running Debian 10. The system contains a 64-bit quad-core processor running at 1.4GHz, with 1GB of ram and a 128GB micro-SD card. Furthermore, besides the included 2.4GHz and 5GHz Wi-Fi 802.11n and Bluetooth 4.1 Low Energy (BLE) (20), a multitude of 40 GPIO pins is present for external communication, providing future extension to other hardware for bio-marker input. Likewise, the Serial Peripheral Interface (**SPI**) communication to the ADC-chip is handled over said GPIO pins. Additionally a 3.5 mm stereo jack is available with PWM-regulated audio playback which currently serves as the main playback module (21). The Raspberry Pi, the main processing hub, controls the different processes of the system. These being then *Process 1a)* capture and *Process 1b)* storage of both internal (EEG) and external bio-markers, *Process 2)* providing analysis of the recorded responses in relation to presented sound and lastly *Process 3)* playback and altering presented sound in a real-time manner to create an engaging and adaptive environment as illustrated in figure 1. Care was expressed in the implementation of said processes here towards ensuring real-time synced accessibility of data and responsiveness of the system in its audio playback. All processes are written and implemented in C, C++ or Python. Furthermore, the measurement data recorded in *Process 1a* is shared between processes and sub-processes through a circular buffer. Here read and write communication is managed by semaphore and read/write indexes onto the circular buffer with implemented overflow and underflow signaling should a process or sub-process lag.

3 Evaluation of the current system

To evaluate performance of the system as a whole, the processes are individually assessed. This being, for *Process 1*, an EEG measurement with comparison to state-of-the-art. *Process 2* and *Process 3* will be evaluated through data-flow observations and overflows in the circular buffer during processing and synchronised playback.

3.1 Process 1 evaluation

The comparison for a proper EEG measurement is made to an ActiveTwo Mk2 BioSemi system (37) in a laboratory setup through an ABR measurement. The reference system captured evoked potentials around the head through active electrodes (sintered Ag-AgCl) operating at 24bit resolution with a sampling rate of 16384Hz and was secured onto the head via a 64 channel Biosemi headcap.

The experiment followed the measurement procedure as outlined in Bleichner et al. (18). Test subjects (5 participants) were positioned inside of a double-walled and electrically shielded listening booth. Each participant took place in a reclining share after which electrodes were attached to the participant's head. For the Biosemi measurement the central-midline electrode Cz (10-20 system) and two earlobe electrodes (EXT1 and EXT2), one placed on each earlobe, are recorded. The common CMS and driven-right-leg (DRL) electrodes were connected to forehead and nose respectively. The Cz measurements were afterwards referenced to the average of EXT1 and EXT2. Alternatively the cEEGrid electrodes were placed around the right ear with a double-sided sticker using the same DRL and CMS positioning serving as main reference. The cEEGrid channels were referenced as well, but to other cEEGrid channels in line with (16). For both electrode setups conductive gel was applied.

The stimuli consisted of 4000 clicks of alternating polarity and presented to the right ear via an in-ear speaker. These clicks occurred at an average rate of 10Hz with a uniformly distributed jitter up to 10% in period. The click itself consisted of an 80μs pulse followed by silence and calibrated to a 100dB peak-equivalent sound pressure level presented inside the outer ear. The clicks and triggers were generated in MATLAB at a sampling rate of 48kHz and stored together with the EEG data for evaluation.

The processing of the ABR results was done offline in Python for both Cz Biosemi measurements and the POC. A low-pass and high-pass 4th order Butterworth filter were applied to the signals with respective cutoff frequencies of 2000Hz and 100Hz. Afterwards 20ms epochs were taken, with the onset corresponding to the trigger signal and epoch removal of the 15% with the highest amplitudes. The latter then being attributed to artifacts of head movement and others. The mean of the remaining epochs along with bootstrapped statistical noise floor and confidence interval of the mean (16), were calculated and are depicted in Figure 2.

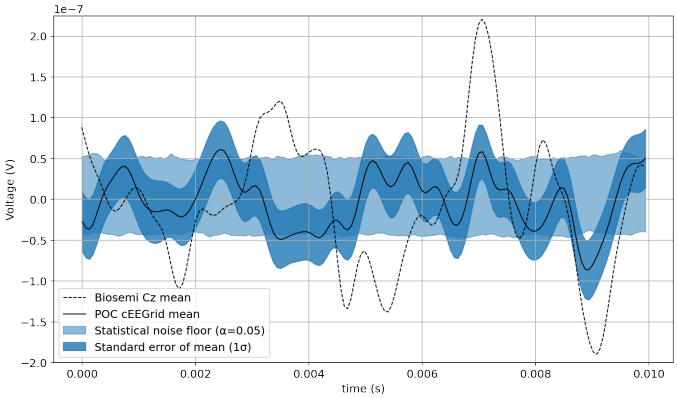

Figure 2. Recorded and processed mean ABR response of 4000 clicks together with its calculated statistical noise floor and standard error of 1 standard deviation for a single subject recorded via the POC and reference Biosemi system.

3.2 Process 2/3 evaluation

To ensure a proper time synced system, both processing and audio playback will be run, managed and maintained in Python to control both time-accurate data processing and audio playback. Here, playback is realised using the Psychtoolbox-3 library inside PsychoPy (36) for Python.

Data processing was evaluated under combined load of both *Process 1a* and *Process 1b* to serve as an initial verification of correct real-time communication under limited load. A time-stamped 0.5s circular buffer was implemented for data-communication and was allocated in the shared memory directory (dev/shm). Furthermore, access to the buffer was restricted through semaphores and checked for discrepancies in data between both

capture and processing. However, an initial verification of data integrity was first performed through comparison of measurement data as stored directly via *Process 1a* as well as though the circular buffer *Process 1b*. This double storage only served as an initial verification of data and the added storage in *Process 1a* was deactivated for all other measurements. A timestamp was furthermore provided every 0.5s for syncing inside the shared memory structure of *Process 1*. The measurement window contained a 400s interval to ensure a full ABR measurement could be performed with a 10Hz stimulation frequency and a maximum of 4000 repetitions, which should moreover be sufficient to capture a full musical interaction with songs of lengths less than 6.5 minutes.

Once content was verified as correctly transferred, overflow in Python is examined under load. Here the readout of the shared circular buffer in *Process 2* into an array was executed by Python while a simple peak detection algorithm ran on the last 1024 recorded values per channel (8 electrode channels from the cEEGrid), serving as initial load. Maximal offset between total written samples to the buffer by *Process 1a* and evaluated samples by *Process 2* was measured over a 400s interval as well.

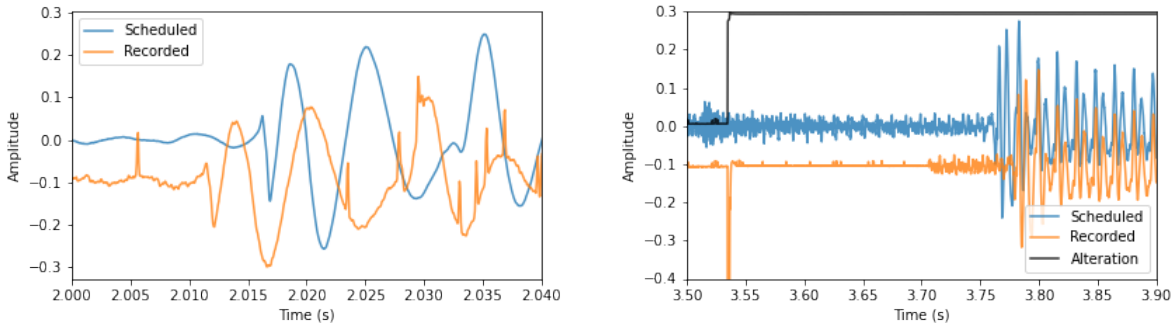

Figure 3. Audio offset and response time illustration, left and right respectively, of the POC. With the original planned audio "Scheduled" and the measured potentials by the ADS-chip "Recorded" and "Alteration".

Evaluation of audio playback is performed to assess both audio consistency of playback as well as responsiveness, i.e. the observed delay to signalled audio changes. As for audio consistency to the internal clock, offset in time between expected presentation time (output through audio jack), based on sample rate and buffer length as predicted by Psychtoolbox, is compared to the arrival time as recorded by the ADS chip. Audio output is directly looped back and connected to the preamplifier input of the system to evaluate the latter offset. Sound production itself was setup with a 4096 sample buffer together with a sample rate of 48kHz. An excerpt was taken from Johnny Nash's "I Can See Clearly Now" as presented audio. The resulting delay for acoustic playback between command execution and sound presentation, based on buffer length and sample rate, should hence not exceed 85.3ms.

Additionally, response time is evaluated between recorded potentials and an associated introduced level change of the presented audio (setting a non-zero amplitude). For the latter a threshold detection was implemented on the recorded potential in Python, which upon activation altered the presented playback level. Figure 3 illustrates both the later recorded audio offset (left) as well as the response time (right). Both figures present scaled versions of presented and recorded signals to increase visibility of the main delays.

4 DISCUSSION AND FUTURE CONSIDERATIONS

4.1 Process 1 EEG acquisition

Comparing the measured EEG responses in Figure 2 to a reference ABR measurement performed as well with cEEGrid (16) similar trends can be observed. Overlaying with the Cz measurement, performed after the cEEGrid measurement to avoid interference, Wave-I, Wave-III and Wave-V can be identified. The latter being characteristic deflections within the first 10ms after stimulus presentation stemming from ascending relay stations of the auditory pathway (22). A clear identifiable Wave-I, Wave-III and Wave-V is present at 2.5ms, 5ms and 7ms

respectively in both measurements. However for the Wave-I, this peak is less visible and seems to be shifted compared to the expected Cz timing, potentially being a consequence of the measurements not being performed simultaneously but in concession. Furthermore, delays as observed are in line with expectations for a 100dB SPL knowing a 1 millisecond audio presentation delay is present in the system (23, 24). Additionally, amplitudes, as observed here for the cEEGrid recording, also agree in magnitude (0.1μV) to the findings in *Garrett et al.* (16). This also applies to the noise floor measurements (+/-0.05μV), which agree with both recorded measurements via the Biosemi system as well as with findings by *Garrett*, hence our proof of concept performs equally well to the latter setup and the Biosemi system. This proof is furthermore backed up by similar results presented in (15).

4.2 Process 2 data processing and storage

Observing then data-flow as a whole within the system, an overall loss-free communication is established between processes. An initial assessment confirmed that a 400s measurement can be recorded between ADS chip and the main computer without a single lost sample for all 8 channels. Real-time data transfer of this collected data was successfully accomplished during a 100s measurement (16kHz, 8 channels) over the cyclic buffer between processes *Process 1a* and *Process 1b*, with a character match for each individual line written to both .txt files before and after the cyclic buffer. The latter confirms a perfect data transmission over the circular buffer.

Extension however to larger measurement intervals caused cyclic buffer overflows and associated loss of data between processes. This is likely a consequence of the limited memory availability under load as the current implementation buffered the full measurement in *Process 1a* for verification here. Alternatively, the continuous write function in *Process 1b* may require too much processing time during recording, resulting in a data overflow in the data collection. Further optimisation to this process as well as a planned hardware upgrade to a Raspberry Pi 4 will likely solve this limitation. Alternatively a binary format storage of the data is considered to avoid redundant bit writing and reduce writing load.

Evaluation under a limited load (only *Process 1a* and no storage *Process 1b*) of Python *Process 2* furthermore illustrated that the system was capable of keeping up with the real-time provided data, acquire and process it from the circular buffer with no loss of data (400s, 8 channels at 16kHz). The amount of read-in unprocessed samples (for each of the 8 read in channels) never exceeded 450 which, translated to time, results in a time-delay of 28.1ms when sampled at 16kHz. As the delay is considerable and comparable in magnitude to the unavoidable delay introduced by the audio-buffer ($\sim$80ms) the prior value was found lacking and currently unacceptable. The combined delay ($\sim$108ms) of both exceeds tolerable values audio music interactions (25) of a maximal 50ms delay and is thus insufficient. A smaller audio-buffer will also be essential here to allow to achieve this 50ms goal which is currently impossible without introducing audible playback glitches.

It should additionally be noted that under the presented limited load, with no storage yet introduced, the communication with the ADS chip suffered from loss of a samples 32 in 6.400.000. The EEG capture can suffer undesired frequency shifts and hence corrupt the measured brain activity data. A 0-loss ADS communication will be aimed for. Further optimisation of resource management along with improved hardware is expected to solve the above mentioned issues and allow perfect communication with the ADS under load.

4.3 Process 3 audio playback

Lastly, regarding audio playback, the offset between planned playback time and actual playtime is illustrated in Figure 3. The offset between both seems to be more or less consistent over time and marginal (5ms) in comparison to the delays introduced by both processing and audio buffering. Nevertheless a compensation of the average offset for said delay will be included in the final audio playback.

In addition the response time, as illustrated in Figure 3, seems to be consistent with the observations made in section **4.2**. A clear time-delay is present between the detection of a high signal by the Python script (Alteration = 0.3), which is situated at 3.54s, and the following change of playback amplitude at 3.71s. Resulting in a total response time of 170ms. Additionally the audio offset seems to have been altered and thus also requires further investigation. Made observations confirm the present delay inside the system between measured response (recorded by the ADS chip) and audio adaptation is currently to high to allow the system to be operated in real time in an adaptive manner compared to the desired 50ms delay (25).

The main limitations of the current proof of concept, being response times above 50ms, sample loss and data buffer overflow, seem to be mainly a consequence of sub-optimal resource management, too large audio buffer and code optimisation. A more efficient file storage (binaries) is aimed to be implemented along with reduced audio-buffer sizes to create more headroom for actual processing. Furthermore, a dedicated core assignment, optimised processing and a hardware improvement into a Raspberry Pi 4 will be implemented. Optionally a dedicated sound card is considered.

5 CONCLUSIONS

In this paper a proof of concept system is presented and evaluated aimed at realising adaptive and interactive music interaction based on recorded EEG data or other biomarkers. The system is currently capable of real-time capture and storage of filtered and digitised EEG data at 16kHz with 8 channels via cEEGrid electrodes up to 400 seconds. A real-time analysis and capture of the EEG data time-synced to presented audio is implemented allowing peak detection and further processing. Moreover, a reliable audio stream at 48kHz is produced by the system capable of adapting playback to real-time captured brain activity. Hardware improvements and code optimisation will be implemented to ensure loss free data capture and lower response time to real time (50ms).

ACKNOWLEDGEMENTS

Work supported by UGENT BOF IOP EarDiMon (WVR), European Research Council ERC-POC 899858 (SV) and FWO-SBO 1SB4421N (AVDB).

REFERENCES

[1] Provasi J, Blanc L, Carchon I. The Importance of Rhythmic Stimulation for Preterm Infants in the NICU. Children (Basel).8(8):660.,2021.

[2] Ashoori A, Eagleman DM, Jankovic J. Effects of Auditory Rhythm and Music on Gait Disturbances in Parkinson's Disease. Front Neurol. 2015;6:234.

[3] Cherko M, Hickson L, Bhutta M. Auditory deprivation and health in the elderly. Maturitas. 2016 Jun;88:52–7.

[4] Münzel T, Sørensen M, Schmidt F, Schmidt E, Steven S, Kröller-Schön S, et al. The Adverse Effects of Environmental Noise Exposure on Oxidative Stress and Cardiovascular Risk. Antioxid Redox Signal. 2018 Mar 20;28(9):873–908.

[5] Haslbeck FB, Jakab A, Held U, Bassler D, Bucher HU, Hagmann C. Creative music therapy to promote brain function and brain structure in preterm infants: A randomized controlled pilot study. Neuroimage Clin. 2020;25:102171.

[6] Fedotchev A, Parin S, Polevaya S, Zemlianaia A. EEG-based musical neurointerfaces in the correction of stress-induced states. Brain-Computer Interfaces. 2022;9(1):1–6.

[7] Leow LA, Watson S, Prete D, Waclawik K, Grahn JA. How groove in music affects gait. Exp Brain Res. 2021 Aug;239(8):2419–33.

[8] Caruso GL, Nijs LL , Leman ML, Hepworth-Sawyer R, Paterson J, Toulson R. 'My avatar and me': technology-enhanced mirror in monitoring music performance practice. In Focal Press - Routledge 2021; 2021. Available from: http://lib.ugent.be/catalog/pug01:8692364.

[9] Collett R, Salisbury I, Loeb RG, Sanderson PM. Smooth or Stepped? Laboratory Comparison of Enhanced Sonifications for Monitoring Patient Oxygen Saturation. Hum Factors. 2020 Feb 1;62(1):124–37.

[10] Filippa M, Panza C, Ferrari F, Frassoldati R, Kuhn P, Balduzzi S, et al. Systematic review of maternal voice interventions demonstrates increased stability in preterm infants. Acta Paediatr. 2017 Aug;106(8):1220–9.

[11] Varni G, Mancini M, Volpe G, Camurri A. A System for Mobile Active Music Listening Based on Social Interaction and Embodiment. Mobile Networks and Applications. 2011;16:375–84.

[12] Rodriguez-Fornells A, Rojo N, Amengual JL, Ripollés P, Altenmüller E, Münte TF. The involvement of audio-motor coupling in the music-supported therapy applied to stroke patients. Ann N Y Acad Sci. 2012 Apr;1252:282–93.

[13] Leman ML, The expressive moment: how interaction (with music) shapes human empowerment [Internet]. Cambridge; 2016. Available from: http://lib.ugent.be/catalog/pug01:8554951.

[14] Martin CP, Glette K, Nygaard TF, Torresen J. Understanding Musical Predictions With an Embodied Interface for Musical Machine Learning. Frontiers in Artificial Intelligence [Internet]. 2020;3. Available from: https://www.frontiersin.org/articles/10.3389/frai.2020.00006.

[15] Van Den Broucke A. Wireless and Wearable EEG Acquisition Hardware Using Around-The-Ear cEEGrid Electrodes. To be published in Proc BIOCAS2022; Taipie, Taiwan. 2022 Oct 13-15.

[16] Garrett M, Debener S, Verhulst S. Acquisition of Subcortical Auditory Potentials With Around-the-Ear cEEGrid Technology in Normal and Hearing Impaired Listeners. Frontiers in Neuroscience [Internet]. 2019;13. Available from: https://www.frontiersin.org/articles/10.3389/fnins.2019.00730.

[17] Bleichner MG, Mirkovic B, Debener S. Identifying auditory attention with ear-EEG: cEEGrid versus high-density cap-EEG comparison. J Neural Eng. 2016 Dec;13(6):066004.

[18] Bleichner MG, Debener S. Concealed, Unobtrusive Ear-Centered EEG Acquisition: cEEGrids for Transparent EEG. Frontiers in Human Neuroscience [Internet]. 2017;11. Available from: https://www.frontiersin.org/articles/10.3389/fnhum.2017.00163.

[19] Espressif Systems. espressif.com. [Online]. Available from: https://espressif.com/sites/default/files/documentation/esp32-datasheet-en.pdf.

[20] Raspberry Pi. raspberrypi.com. [Online]. Available from: https://www.raspberrypi.com/products/raspberry-pi-3-model-b/.

[21] Raspberry Pi. raspberrypi.org. [Online]. Available from: https://static.raspberrypi.org/files/product-briefs/Raspberry-Pi-Model-Bplus-Product-Brief.pdf.

[22] Melcher JR, Kiang NY. Generators of the brainstem auditory evoked potential in cat. III: Identified cell populations. Hear Res. 1996 Apr;93(1–2):52–71.

[23] Lewis JD, Kopun J, Neely ST, Schmid KK, Gorga MP. Tone-burst auditory brainstem response wave V latencies in normal-hearing and hearing-impaired ears. The Journal of the Acoustical Society of America. 2015 Nov;138(5):3210—3219.

[24] Verhulst S, Jagadeesh A, Mauermann M, Ernst F. Individual Differences in Auditory Brainstem Response Wave Characteristics: Relations to Different Aspects of Peripheral Hearing Loss. Trends Hear. 2016 Nov 11;20.

[25] Chew E, SAWCHUK A, Kyriakakis C, Papadopoulos C, François A, Volk A, et al. DISTRIBUTED IMMERSIVE PERFORMANCE. 2022 Jul 15.

[26] Sihvonen AJ, Särkämö T, Leo V, Tervaniemi M, Altenmüller E, Soinila S. Music-based interventions in neurological rehabilitation. Lancet Neurol. 2017 Aug;16(8):648–60.

[27] Benoit CE, Dalla Bella S, Farrugia N, Obrig H, Mainka S, Kotz SA. Musically Cued Gait-Training Improves Both Perceptual and Motor Timing in Parkinson's Disease. Frontiers in Human Neuroscience [Internet]. 2014;8. Available from: https://www.frontiersin.org/articles/10.3389/fnhum.2014.00494.

[28] Kadivar Z, Corcos DM, Foto J, Hondzinski JM. Effect of step training and rhythmic auditory stimulation on functional performance in Parkinson patients. Neurorehabil Neural Repair. 2011 Sep;25(7):626–35.

[29] Dieringer ST, Porretta DL, Sainato D. Music and On-task Behaviors in Preschool Children With Autism Spectrum Disorder. Adapt Phys Activ Q. 2017 Jul;34(3):217–34.

[30] Finnigan E, Starr E. Increasing social responsiveness in a child with autism. A comparison of music and non-music interventions. Autism. 2010 Jul;14(4):321–48.

[31] Croom AM. Music practice and participation for psychological well-being: A review of how music influences positive emotion, engagement, relationships, meaning, and accomplishment. Musicae Scientiae. 2015 Mar 1;19(1):44–64.

[32] Buhmann J, Desmet F, Moens B, Van Dyck E, Leman M. Spontaneous Velocity Effect of Musical Expression on Self-Paced Walking. PLOS ONE. 2016 May 11;11(5):e0154414.

[33] Moens B, Muller C, van Noorden L, Franěk M, Celie B, Boone J, et al. Encouraging Spontaneous Synchronisation with D-Jogger, an Adaptive Music Player That Aligns Movement and Music. PLOS ONE. 2014 Dec 9;9(12):e114234.

[34] Sourina O, Liu Y, Nguyen MK. Real-time EEG-based emotion recognition for music therapy. Journal on Multimodal User Interfaces. 2012 Mar 1;5(1):27–35.

[35] Yuksel, Beste Filiz, Afergan, Daniel, Peck, Evan, Griffin, Garth, Harrison, Lane, Chen, Nick, et al. BRAAHMS: A Novel Adaptive Musical Interface Based on UsersĆognitive State. In: Proceedings of the International Conference on New Interfaces for Musical Expression. Zenodo; 2015. p. 136–9

[36] PsychoPy. [Online]. Available from: https://www.psychopy.org/.

[37] Biosemi. [Online]. Available from: https://www.biosemi.com/activetwo_full_specs.htm.

[38] Dasenbrock S, Blum S, Debener S, Hohmann V, Kayser H. A Step towards Neuro-Steered Hearing Aids: Integrated Portable Setup for Time- Synchronized Acoustic Stimuli Presentation and EEG Recording. Current Directions in Biomedical Engineering. 2021;7(2): 855-858.

24th INTERNATIONAL CONGRESS ON ACOUSTICS

ICA 2022

October 24(Mon) - 28(Fri), 2022 | Gyeongju, Korea

PROCEEDINGS

Hosted by The Acoustical Society of Korea | ICA